Published in final edited form as:
J Cardiovasc Electrophysiol. 2010 December ; 21(12): 1365–1372. doi:10.1111/j.1540-8167.2010.01844.x.

A NOVEL MUTATION IN THE HCN4 GENE CAUSES SYMPTOMATIC SINUS BRADYCARDIA IN MOROCCAN JEWS

Avishag Laish-Farkash, MD, PhD[*], **Dovrat Brass, PhD**[‡], **Dina Marek-Yagel, MSc**[†], **Elon Pras, MD**[†], **Nathan Dascal, PhD**[‡], **Charles Antzelevitch, PhD**[§], **Eyal Nof, MD**[*], **Haya Reznik, PhD**[†], **Michael Eldar, MD**[*], **Michael Glikson, MD**[*], and **David Luria, MD**[*]

[*] Heart Institute, Sheba Medical Center, Tel Hashomer

[†] Laboratory of Human Genetics, Sheba Medical Center, Tel Hashomer

[‡] Department of Physiology and Pharmacology, Sackler Faculty of Medicine, Tel Aviv University, Tel Aviv, Israel

[§] Masonic Medical Research Molecular Biology Laboratory (MMRL), Utica NY, USA

Abstract

Objectives—To conduct a clinical, genetic and functional analysis of three unrelated families with familial sinus bradycardia (FSB).

Background—Mutations in the hyperpolarization-activated nucleotide-gated channel (*HCN4*) are known to be associated with FSB.

Methods and Results—Three males of Moroccan Jewish descent were hospitalized: one survived an out-of-hospital cardiac arrest and 2 presented with weakness and presyncopal events. All 3 had significant sinus bradycardia, also found in other first-degree relatives, with a segregation suggesting autosomal-dominant inheritance. All had normal response to exercise and normal heart structure.

Sequencing of the *HCN4* gene in all patients revealed a C to T transition at nucleotide position 1454, which resulted in an alanine to valine change (A485V) in the ion channel pore found in most of their bradycardiac relatives, but not in 150 controls. Functional expression of the mutated ion channel in *Xenopus* oocytes and in human embryonic kidney 293 cells revealed profoundly reduced function and synthesis of the mutant channel compared to wild-type.

Conclusions—We describe a new mutation in the *HCN4* gene causing symptomatic FSB in 3 unrelated individuals of similar ethnic background that may indicate unexplained FSB in this ethnic group. This profound functional defect is consistent with the symptomatic phenotype.

Keywords

electrophysiology; genetics; heart rate; ion channels

Hyperpolarization-activated, cyclic nucleotide-gated (*HCN*) channels are voltage-gated ion channels activated in hyperpolarized membrane potential that mediate the hyperpolarization-evoked pacemaker (“funny”) current (I_f) in the heart. I_f is a nonselective cationic inward current that contributes significantly to spontaneous diastolic membrane depolarization of sinoatrial node cells (1–4). *HCN* channels are thought to be key players in generating and

Correspondence: David Luria, M.D., Heart Institute, Sheba Medical Center, 52621 Tel Hashomer, Israel, Tel: 972-3 5302683, 972-3 5305252, Fax: 972-3 5343888, dluria@sheba.health.gov.il.
The first two authors (A.L-F. and D.B.) contributed equally to this work.

regulating pacemaker activity (5–8). Of the four known *HCN* subunits, *HCN4* is the most highly expressed in the mammalian sinoatrial node (9–12). Mutations in gene encoding for *HCN4* channel account for inherited sinus bradycardia (13–16). So far, four different heterozygous HCN4 mutated channels have been identified in humans. The mutations are 573X (14), D553R (15), S672R (13) and G480R (16). The two last mutations activate at voltages more negative than wild-type (WT) channels, decreasing inward diastolic depolarization current thereby slowing heart rate (13,15–16).

We describe 3 families of Moroccan Jewish descent with symptomatic familial sinus bradycardia (FSB) and a common mutation in gene coding for the *HCN4* channel. We hypothesize that resultant combined defects in channel characteristics and synthesis might influence the clinical phenotype.

Methods

Patient population

Family pedigrees are presented in Figure 1. Twenty members from three families of Moroccan decent were evaluated: 13 from family A; 6 from family H; and 1 member from family V. All patients gave informed consent approved by the Institutional Ethics Committee of the Sheba Medical Center

Evaluation included a clinical questionnaire, resting ECG, and 24-hour Holter monitoring, interpreted via a computerized system (Impresario 3.04.0089, DELMAR systems, Irvine, Calif) and confirmed by an electrophysiologist. Two-dimensional echocardiography was performed in 8 carriers and 5 noncarriers, and treadmill exercise tests were performed in 8 carriers and 4 noncarriers.

The definition of an affected family member was based on minimum heart rates of ≤40 or average heart rate ≤60 bpm during Holter monitoring. Repeated sinus bradycardia on ECG recording was taken to consideration.

Genetic analysis

DNA was extracted with a commercial kit (Gentra System Inc, Minneapolis, Minn), and primers were designed with Primer3 software (17). The whole coding region and exon-intron boundaries of *HCN4* were amplified and sequenced as previously described (14). Alanine to valine change (A485V) mutation was confirmed with a restriction assay. The mutation-containing segment was amplified with primers 5′-agttaggttgaggaggtg-3′ and 5′-ctcttccctcacactgggagtt-3′ in a 25-μL reaction containing 50 ng DNA, 13.4 ng each primer, 1.5 mmol/L dNTPs, 1.5 mmol/L MgCl2, and polymerase chain reaction buffer, with 1.2 U Taq polymerase (Bio-Line, London, UK). After an initial 5-minute denaturation period at 95°C, 30 cycles were performed (94°C for 30 seconds, 58°C for 30 seconds, and 72°C for 30 seconds), followed by a final extension of 10 minutes at 72°C. The amplification product was then cut with the *EheI* restriction enzyme (Fermentas). A control group of 150 healthy subjects was used to assess mutation frequency.

Molecular cloning of HCN4 and in Vitro RNA synthesis

Human HCN4 cDNA in pCDNA3 vector (*hHCN4*; accession No. AJ132429) was provided by Dr F. Hofmann (Technical University of München, Germany). The HCN4 A485V point mutation was introduced using the QuickChange Site-Direct Mutagenesis Kit (Stratagene, La Jolla, Calif) into pCDNA3 as well as pGEM-HJ vectors. All mutations and polymerase chain reaction products were verified by direct sequencing. For *Xenopus* oocyte expression, the RNAs were prepared using standard procedures, which ensured capping the 5′ end of the

RNA and preferential inclusion of noncapped GTP in the remaining RNAs (18). Before transcription, the plasmid DNA was linearized with *Nhe*I.

Oocyte culture and electrophysiology

Xenopus laevis frogs (Xenopus I, Dexter, Mich) were maintained and operated on, and oocytes were collected, defolliculated and injected with RNA as described (19). The oocytes were injected with RNAs of *HCN4* WT (2.5 ng/oocyte), *HCN4* A485V (2.5 ng/oocyte), or *HCN4* WT/A485V (1.25 ng each per oocyte) mRNA and incubated as previously described by our group (16). Whole-cell currents were recorded by a Gene Clamp 500 amplifier (Axon Instruments, Foster City, Calif) using the two-electrode voltage clamp technique (20). The pipette solution contained 3 mol/L KCl.

Human embryonic kidney 293 cell culture and electrophysiology

Human embryonic kidney 293 cells (HEK293T) were cultured and transfected as described (16), with similar DNA amounts used per 24-well dish.

Patch-clamp experiments were performed 24 hours after transfection. Membrane currents were recorded under voltage-clamp conditions using conventional whole-cell patch-clamp techniques. Whole cell patch-clamp recordings were performed as described (16). A pCLAMP software package was used for voltage control, data acquisition, and data evaluation.

Western blot analysis of HEK293T cells

HEK293T cells were transfected, grown and further homogenized in lysis buffer as previously described (16).

Presentation and analysis of the experimental results

Electrophysiological data were analyzed with pCLAMP9 software (Axon Instruments), SigmaPlot 2000, and SigmaStat (both SPSS Inc.) Data are presented as mean±SEM. A 2-tailed unpaired *t* test was used to compare differences between the 2 groups. One-way ANOVA, followed by Dunnett or Tukey tests, were used for comparison between several groups.

Results

Index patients

The first patient, a healthy 21-year-old male (Fig 1B, arrow), survived out-of-hospital cardiac arrest during extreme exercise. After cardiopulmonary resuscitation (CPR) with basic life support but no DC cardioversion, spontaneous circulation returned, but he remained unconscious. The first rhythm observed on monitor recordings after CPR was narrow complex tachycardia. Slow neurologic recovery was observed thereafter and he was discharged at cerebral performance category grade 1. During hospitalization, a baseline sinus bradycardia (SB) rhythm was noted. Holter monitoring showed baseline SB without conduction defects or arrhythmias. 2D-echocardiography, cardiac computerized tomography(CT) and magnetic resonance imaging (MRI), adenosine test, epinephrine test and flecainide test, brain CT and MRI, electroencephalogram (EEG) and EEG after sleep deprivation revealed no abnormal findings. Electrophysiological study revealed only inducible atrial fibrillation and typical flutter without rapid ventricular response. An exercise test demonstrated good functional capacity and preserved chronotropic reserve without arrhythmia during exercise. Genetic screening for *SCN5A*, *HERG*, *HCN4*, *KCNJ2*, *KCNJ3*,

KCNJ5 and *KCNQ1*, *KCNH2*, and *KCNJ12* found no mutations in these genes. The patient refused ICD implantation and had no clinical events during a 2-year follow-up.

The second patient, a 21-year-old male (Fig. 1A, arrow), was admitted to the electrophysiology unit complaining of fatigue, weakness and presyncopal events. The third patient, a 50-year-old male (Fig. 1C, arrow), was admitted due to symptomatic paroxysmal atrial fibrillation. Baseline ECG and Holter recordings in both patients showed significant SB, also found in several other first-degree family members. Echocardiography and exercise tests were within normal limits. Further questioning revealed that the families of all 3 patients immigrated to Israel from the same city, Casablanca Morocco,.

HCN4 screening

Sequencing of the whole coding region and intron boundaries of the *HCN4* gene in 2 patients revealed a heterozygote C to T transition at position 1454 (exon 4) that resulted in the substitution of alanine to valine at position 485 in the protein (A485V) (Fig. 2A). This change abolished an *EheI* restriction site in the patients, and therefore we used restriction digests to detect the mutation in other patients, family members and controls. The mutation was not found in 150 controls (100 of Moroccan origin). Multiple alignments in different species show a conserved alanine at this position (Fig. 2B).

Family members

After completion of the 24-hour Holter monitoring, 14 family members were initially classified as affected (Fig 1D). Repeated ECG recordings consistently documented SB in these patients. Only one of them (A-III-2), an asymptomatic athletic young female, was later found to be a noncarrier and thus representing a phenocopy. Fourteen family members were found to be carriers of the A485V (Table 1). Carriers and noncarriers of the mutation were at similar age but had significantly different minimum and average heart rate (Table 2).

Most, but not all, mutation carriers were bradycardic and complained of dizziness and presyncopal events. Family member H-III-2, a carrier of the mutation, had profound sinus bradycardia on the rest ECG since childhood, but displayed borderline Holter results during current recording and was completely asymptomatic.

There were no other rhythm or conduction abnormalities, except for family member V-II-2, who presented with paroxysmal atrial fibrillation at the age of 50. QTc was within normal limits in all participants (381±28 ms). Except for one index patient (H-III-3), there were no other cases of sudden cardiac death in any of the families. Exercise testing demonstrated normal chronotropic and exercise capacity without any conduction disturbances or arrhythmias (Table 1); echocardiography revealed a normally-structured heart in all tested family members.

Functional expression of HCN4 WT and A485V mutant in *Xenopus* oocytes

A two-electrode voltage clamp was used to investigate functional change caused by the A485V mutation. A485V was expressed alone (to mimic the homotetramer phenotype) or with WT (to mimic the heterotetramer phenotype). In oocytes injected with WT *HCN4* RNA, 5-s hyperpolarizing steps from −30 mV elicited slow-activating inward currents at voltages below −65 mV, typical for *HCN4* I_f current(Figure 3A–C). Increase in current amplitude and time course of current activation pattern of the A485V homotetramer and heterotetramer states differed significantly from the WT *HCN4*. The A485V homotetramer currents were apparent only below −120 mV, and developed much more slowly than in the WT (Fig. 3A–C). In contrast, the WT/A485V heterotetramer currents were apparent below −80 mV, while developing more slowly than in the WT but faster than the A485V

homotetramer (Fig. 3A–C). No significant differences were found in the reversal potential (~ −10mV) (Fig. 3D). The A485V and WT/A485V heterotetramer tail currents obtained during the voltage step to 30 mV had much slower deactivation kinetics (Figure 3B).

Functional expression of the *HCN4* channel containing A485V point mutation, compared to the G480R mutant channel identified recently (16), revealed that the A485V and G480R homotetramer currents recorded at −80 mV were both significantly reduced compared to the WT (relative to the WT current recorded in the same experiment) (Figure 4). The differences are much higher at −120 mV, in which the A485V homotetramer current constitute ~ 2.5% of the WT current, whereas the G480R homotetramer current constitute ~ 20% of the WT current (Figure 4).

Synthesis of WT and A485V HCN4 channels

Western blot analysis of total *HCN4* protein in HEK293T cells revealed significantly reduced expression of homomeric *HCN4* A485V channels in the cells. The total amount of mutated A485V channel protein, compared to WT channel protein, was significantly altered in two different experiments (Figure 5). Calnexin levels, which served as a protein control for the Western blot analysis, were similar in cells expressing A485V mutant and WT channels. *HCN4* protein was not detected in pCDNA3-transfected HEK293T cells.

Functional expression of HCN4 WT and A485V mutant in HEK293T cells

A whole-cell patch-clamp recording was used in HEK293T cells to investigate functional changes caused by the A485V mutation in mammalian cells. As in the oocytes expression system, the current amplitude and time course of the current activation pattern of the homotetramer A485V mutated channel state were strikingly different from the WT *HCN4* (Fig. 5B). Cells expressing *HCN4* A485V channel protein showed leak current elevation (recorded between −30 to −60 mV), as well as closure of an unknown channel at highly negative voltages. Other cells expressing *HCN4* A485V showed no current. In conclusion, no *HCN4* characteristic current was seen in any of the HEK293T cells expressing the A485V protein. Consequently, the current density of the A485V mutant channel at −100 mV was significantly reduced compared to the WT *HCN4* transfected HEK293T cells.

Discussion

We describe a new mutation, A485V, in the *HCN4* gene in 3 patients of Moroccan Jewish descent with symptomatic FSB. The existence of this mutation in 3 individuals from the same ethnic group, originating from the same town, suggests a founder effect and implies it might underlie a relatively common cause for unexplained congenital SB in this ethnic group. Similar to other FSB family reports (15–16,21–22), the inheritance mode in our affected families is autosomal dominant (Figure 1).

Previously known *HCN4* channel mutations causing FSB were localized in the intracellular C-terminus region (13–15). The A485V is the second mutation located in the pore region described to cause FSB, but in this case, unlike the previously identified G480R pore-region mutation, the mutated amino acid lies outside the selectivity filter.

In contrast to G480R, which caused asymptomatic FSB (16), most of the A485V carriers were symptomatic at varying degrees (dizziness, presyncopal episodes, albeit without slower heart rate - Table 2) and one index patient had out-of-hospital cardiac arrest during extreme exercise (the initial arrhythmia was not recorded). Although we cannot prove that *HCN4* abnormality was involved in the pathogenesis of a dangerous arrhythmia or sinus arrest in this case, no mutations were found in this young man in other genes known to cause sudden cardiac death, and a previous trafficking-defective *HCN4* mutation, D553N, was already

found to be associated with lethal cardiac arrhythmia (15). In addition, in a recent study by Herrmann et al (23), deletion of *HCN4* in adult mice eliminated most of sinoatrial If and resulted in cardiac arrhythmia characterized by recurrent long sinus pauses.

The genetic aspect

Several lines of evidence suggest that the A485V substitution has functional consequences and is not just a silent polymorphism. First, it was not found in 150 controls, of whom100 were of Moroccan origin. Second, the change occurred in a segment highly preserved throughout evolution. Third, this substitution caused a functional electrophysiological change that underlies the clinical phenotype.

Proposed mechanism of inherited sinus bradycardia in affected families

We report here a new A485V mutation in the *HCN4* protein, located in the loop connecting the pore to the S6 segment that affects the channel gating. Several studies have demonstrated the significant influence of point mutations in GYG sequence on *HCN* channel gating, suggesting that, although this part of the pore may be involved in governing selectivity, it also substantially controls gating (24,25). However, to date no data exist regarding the contribution of the surrounding amino acids, near the *HCN4* channel pore, to the gating.

The A485V mutation, as in the former identified G480R mutation, showed a significant reduction in mutated channel protein synthesis, compared to the WT. A significant reduction in the synthesis of the *HCN4* A485V channel was observed compared to the WT (Figure 5). This impairment in synthesis and bioprocessing probably explains the radically reduced current amplitude, both in HEK cells and oocytes. However, it appears that a greater percentage of mutant channels escaped the ER quality control and reached the plasma membrane in the oocytes, as compared to HEK cells, possibly because of the lower incubation temperature.

The presence of a residual current in *Xenopus* oocytes allowed a partial electrophysiological analysis, revealing a similarity in the reversal potential of *HCN4* WT and A485V mutant channels, suggestive of similar ion selectivity (Figure 3D). However, the gating was greatly changed: the A485V homotetramer *HCN4* activation curves shifted to markedly more hyperpolarized potentials relative to the WT *HCN4* (Figure 3A–C), resulting in a significantly reduced current at physiologically relevant voltages of activation (between −60 and −90 mV). There was also a shift in heterotetramer activation curves to a more hyperpolarized potential. However, heterotetramer current reduction, relative to the WT, was less significant (Figure 3A–C). The physiologically relevant component of activation (between −60 and −90 mV), present in the WT channels, was absent in the homotetrameric mutant and reduced in the WT/A485V heterotetramer. The reduced protein expression, as well as the more negative range of activation in this *HCN4* mutant, concur with the reduced contribution of the mutated channel in physiological conditions to the I_f current.

According to the oocyte data, the A485V mutant probably forms heterotetrameric channels, when co-expressed with WT channels, since the I_f current in oocytes injected with a mixture of the corresponding RNAs, has a reduced amplitude, and its I–V curve is shifted to more negative voltages compared with WT (since I_f homotetrameric WT channels in these cells are expressed separately, one would expect a component of the total current to have a normal I–V curve). Thus, we surmise that heterotetrameric channels containing the A485V mutation have an altered gating, combined with poorly synthesis in the cell. Conseuqently, they probably do not contribute to the I_f current in atrial myocytes. We cannot exclude the possibility of a trafficking impairment of the mutated channel to the plasma membrane, which might influence the clinical phenotype as well. The heterozygous expression of the

affected Moroccan family members may not confer the same properties as the heterozygous expression in heterologous cells.

The fact that the mutation carriers demonstrated normal chronotropic and exercise capacity during exercise test, despite the combined synthesis defects and altered biophysical properties of the mutant A485V HCN4 channels, may strengthen the minor contribution of the *HCN4* current to the overall I_f current in the heart, or suggest that the functional importance of HCN4 might be different, as reported by Herrmann S et al (23). They showed that deletion of HCN4 in adult mice eliminated most of sinoatrial I_f and resulted in a cardiac arrhythmia characterized by recurrent sinus pauses. However, the mutants showed no impairment in heart rate acceleration during sympathetic stimulation. These results suggested that the HCN4 channel is not critical for proper acceleration of the heart rate; however, HCN4 is necessary for maintaining a stable cardiac rhythm, especially during the transition from stimulated to basal cardiac states. The newly described mechanisms, independent of I_f current, such as intracellular calcium cycling, involving ryanodine receptors, L-type calcium channels and the sodium –calcium exchanger may be involved in catecholamine dependent heart rate stimulation.

Another possibility is the formation of HCN4 WT/HCN4A485V channel in heterozygous patients. The HCN4 mutations detected in human patients are heterozygous mutations and no deletions; that is, there is still one intact allele. I_f, or rather HCN4 currents in these patients are therefore not deleted, but differently modulated, which could result in quite different effects than a complete lack of the current. Alternatively, one may speculate that there might be compensation for the impaired mutated channel protein by heteromerization with *HCN2* (the dominant mRNA transcripts in atrial myocardium (26)). This mechanism was previously suggested by Zha et al for *HCN1* and *HCN2* in the brain (27).

Clinical implications

Familial sinus bradycardia may require pacemaker implantation because of extremely low heart rate, long-QT, or ventricular arrhythmia related to bradycardia (28–30). We have no proof of direct cause and effect of the A485V mutation on the cardiac arrest experienced byone of our index patients. We have no evidence that the genetic defect was somehow related to the cardiac arrest, and since we have no similar cases in this family or in other families, the reason for the severe clinical manifestation in this case remains obscure. At present, our remaining mutation carriers show a mild phenotype that does not justify any intervention. Future decision regarding implantation of a pacemaker should be guided by the severity of symptoms. Further follow-up and data collection could clarify risk stratification for carriers of this new mutation.

Acknowledgments

Dr. Laish-Farkash received support from an Israel Heart Society Scholarship for Medical Research. Dr. Antzelevitch reports research support from NHLBI HL47678.

Abbreviations

2D-echocardiography	two-dimensional echocardiography
CPR	cardio-pulmonary resuscitation
CT	computerized tomography
EEG	electroencephalogram
FSB	familial sinus bradycardia

HCN	Hyperpolarization-activated, cyclic nucleotide-gated channel
HEK293T	Human embryonic kidney 293 cells
I_h or I_f	hyperpolarization-evoked pacemaker (“funny”) current
MRI	Magnetic Resonance Imaging
SB	sinus bradycardia
WT	wild-type

References

1. Stieber J, Herrmann S, Feil S, et al. The hyperpolarization-activated channel HCN4 is required for the generation of pacemaker action potentials in the embryonic heart. Proc Natl Acad Sci U S A. 2003; 100:15235–15240. [PubMed: 14657344]
2. DiFrancesco D, Tortora P. Direct activation of cardiac pacemaker channels by intracellular cyclic AMP. Nature. 1991; 351:145–147. [PubMed: 1709448]
3. DiFrancesco D. Pacemaker mechanisms in cardiac tissue. Annu Rev Physiol. 1993; 55:455–472. [PubMed: 7682045]
4. Baruscotti M, Bucchi A, DiFrancesco D. Physiology and pharmacology of the cardiac pacemaker (“funny”) current. Pharmacol Ther. 2005; 107:59–79. [PubMed: 15963351]
5. Ludwig A, Zong X, Jeglitsch M, Hofmann F, Biel M. A family of hyperpolarization-activated mammalian cation channels. Nature. 1998; 393(6685):587–91. [PubMed: 9634236]
6. Kaupp UB, Seifert R. Molecular diversity of pacemaker ion channels. Annu Rev Physiol. 2001; 63:235–257. Review. [PubMed: 11181956]
7. Biel M, Schneider A, Wahl C. Cardiac HCN channels: structure, function, and modulation. Trends Cardiovasc Med. 2002; 12:206–12. Review. [PubMed: 12161074]
8. Robinson RB, Siegelbaum SA. Hyperpolarization-activated cation currents: from molecules to physiological function. Annu Rev Physiol. 2003; 65:453–80. Review. [PubMed: 12471170]
9. Ishii TM, Takano M, Xie LH, Noma A, Ohmori H. Molecular characterization of the hyperpolarization-activated cation channel in rabbit heart sinoatrial node. J Biol Chem. 1999; 274:12835–12839. [PubMed: 10212270]
10. Shi W, Wymore R, Yu H, et al. Distribution and prevalence of hyperpolarization-activated cation channel (HCN) mRNA expression in cardiac tissues. Circ Res. 1999; 85(1):e1–6. [PubMed: 10400919]
11. Moosmang S, Stieber J, Zong X, Biel M, Hofmann F, Ludwig A. Cellular expression and functional characterization of four hyperpolarization-activated pacemaker channels in cardiac and neuronal tissues. Eur J Biochem. 2001; 268(6):1646–52. [PubMed: 11248683]
12. Liu J, Dobrzynski H, Yanni J, Boyett MR, Lei M. Organisation of the mouse sinoatrial node: structure and expression of HCN channels. Cardiovascular Res. 2007; 73:729–738.
13. Milanesi R, Baruscotti M, Gnecchi-Ruscone T, DiFrancesco D. Familial sinus bradycardia associated with a mutation in the cardiac pacemaker channel. N Engl J Med. 2006; 354:151–157. [PubMed: 16407510]
14. Schulze-Bahr E, Neu A, Friederich P, Kaupp UB, Breithardt G, Pongs O, Isbrandt D. Pacemaker channel dysfunction in a patient with sinus node disease. J Clin Invest. 2003; 111:1537–1545. [PubMed: 12750403]
15. Ueda K, Nakamura K, Hayashi T, et al. Functional characterization of a trafficking-defective HCN4 mutation, D553N, associated with cardiac arrhythmia. J Biol Chem. 2004; 279:27194–27198. [PubMed: 15123648]
16. Nof E, Luria D, Brass D, et al. Point mutation in the HCN4 cardiac ion channel pore affecting synthesis, trafficking, and functional expression is associated with familial asymptomatic sinus bradycardia. Circulation. 2007; 116:463–470. [PubMed: 17646576]

17. [Accessed March 30, 2006]. Available at: http://frodo.wi.mit.edu/cgi-bin/primer3/primer3_www.cgi
18. Yamada M, Inanobe A, Kurachi Y. G protein regulation of potassium ion channels. Pharmacol Rev. 1998; 50:723–60. [PubMed: 9860808]
19. Dascal, N.; Lotan, I. Expression of exogeneous ion channels and neurotransmitter receptors in RNA-injected Xenopus oocytes. In: Longstaff, A.; Revest, P., editors. Protocols in Molecular Neurobiology. Vol. 13. Humana Press; Totowa, NJ, USA: 1992. p. 205-225.
20. Lim NF, Dascal N, Labarca C, Davidson N, Lester HA. A G protein-gated K channel is activated via beta 2-adrenergic receptors and G beta gamma subunits in Xenopus oocytes. J Gen Physiol. 1995; 105:421–39. [PubMed: 7769382]
21. Lorber A, Maisuls E, Palant A. Autosomal dominant inheritance of sinus node disease. Int J Cardiol. 1987; 15:252–256. [PubMed: 3583465]
22. Mehta AV, Chidambaram B, Garrett A. Familial symptomatic sinus bradycardia: autosomal dominant inheritance. Pediatr Cardiol. 1995; 16:231–234. [PubMed: 8524708]
23. Herrmann S, Stieber J, Stockl G, Hofmann F, Ludwig A. HCN4 provides ‘depolarization reserve’ and is not required for heart rate acceleration in mice. EMBO J. 2007; 26:4423–4432. [PubMed: 17914461]
24. Azene EM, Xue T, Li RA. Molecular basis of the effect of potassium on heterologously expressed pacemaker (HCN) channels. J Physiol. 2003; 547:349–356. [PubMed: 12562911]
25. Macri V, Proenza C, Agranovich E, Angoli D, Accili EA. Separable gating mechanisms in a Mammalian pacemaker channel. J Biol Chem. 2002; 277:35939–35946. [PubMed: 12121985]
26. Ludwig A, Zong X, Stiber J, Hullin R, Hofmann F, Biel M. Two pacemaker channels from human heart with profoundly different activation kinetics. EMBO J. 1999; 18:2323–2329. [PubMed: 10228147]
27. Zha Q, Brewster AL, Richichi C, Bender RA, Baram TZ. Activity-dependent heteromerization of the hyperpolarization-activated, cyclic-nucleotide gated (HCN) channels: role of N-linked glycosylation. Journal of Neurochemistry. 2008; 105:68–77. [PubMed: 17988239]
28. Albin G, Hayes DL, Holmes DR Jr. Sinus node dysfunction in pediatric and young adult patients: treatment by implantation of a permanent pacemaker in 39 cases. Mayo Clin Proc. 1985; 60:667–672. [PubMed: 4033231]
29. Beder SD, Gillette PC, Garson A Jr, Porter CB, McNamara DG. Symptomatic sick sinus syndrome in children and adolescents as the only manifestation of cardiac abnormality or associated with unoperated congenital heart disease. Am J Cardiol. 1983; 51:1133–1136. [PubMed: 6837459]
30. Gulotta SJ, Gupta RD, Padmanabhan VT, Morrison J. Familial occurrence of sinus bradycardia, short PR interval, intraventricular conduction defects, recurrent supraventricular tachycardia, and cardiomegaly. Am Heart J. 1977; 93:19–29. [PubMed: 137666]

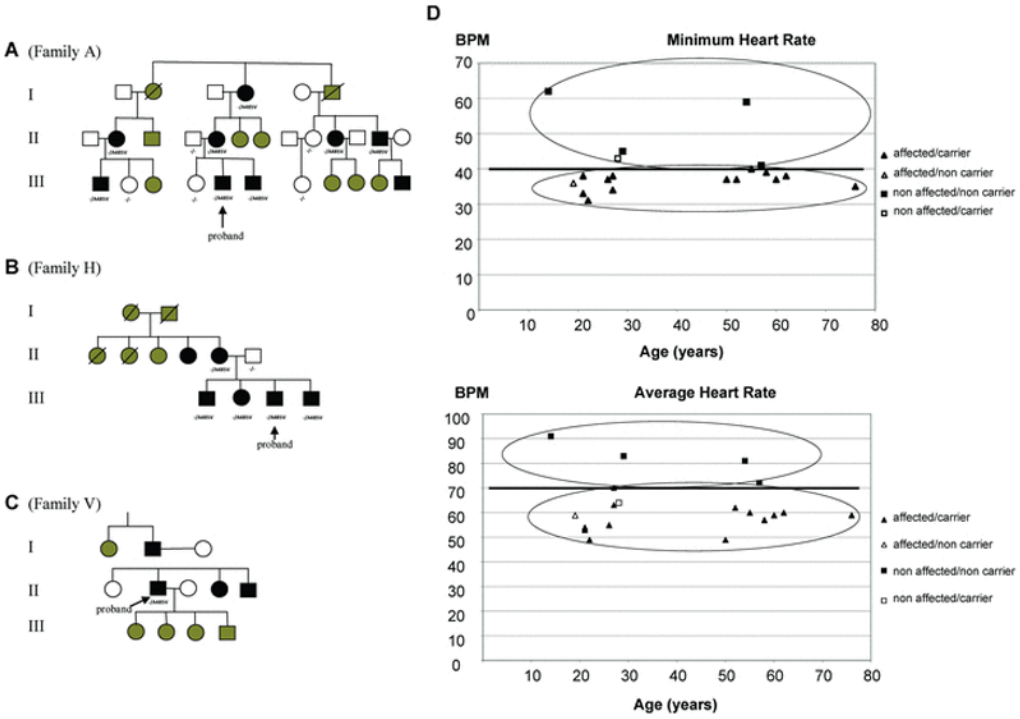

Figure 1. Family members

A–C. Family trees suggesting autosomal-dominant inheritance. Solid symbols represent affected family members. Open symbols indicate family members not carrying the mutant gene. Gray symbols represent patients whose clinical and genetic status is unknown. (Patients A-III-11, H-II-4, V-I-2, V-II-4, and V-II-5 were considered affected based only on a history of bradycardia without genetic screening due to lack of cooperation. Patients A-I-2 and A-I-6 died at 28y from unknown causes).

D. This chart compares age with heart rate of carrier- and noncarrier family members. It demonstrates clear separation of two groups: affected and nonaffected family members, regarding minimal and mean heart rate on Holter recordings, independently of patient age. Low heart rate segregates near completely with positive genotype. Two exceptions are discussed in the text. Family member A-II-9 was not included in the graph due to technically unreadable Holter recordings. She was asymptomatic and was found to be a noncarrier.

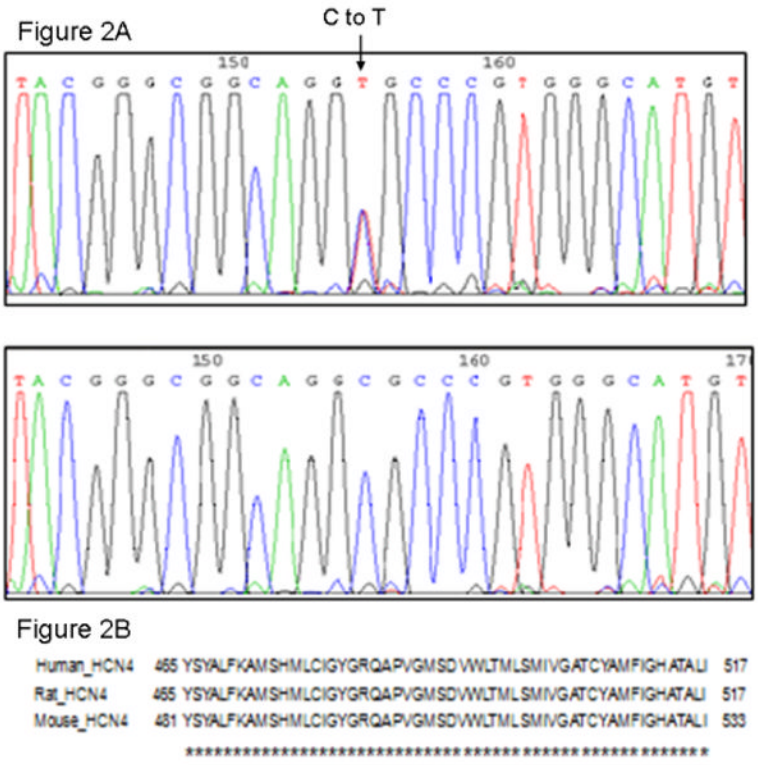

Figure 2. The A485V mutation

A. Top: In this patient a C to T heterozygote change resulted in an alanine to valine amino acid change in position 485. **Bottom**: Control showing normal sequence. **B.** Multiple alignment of the A485V mutation region, showing the conserved alanine in position 485 in 3 different species (human, rat and mouse). The multiple alignment was done using the ClustalW software.

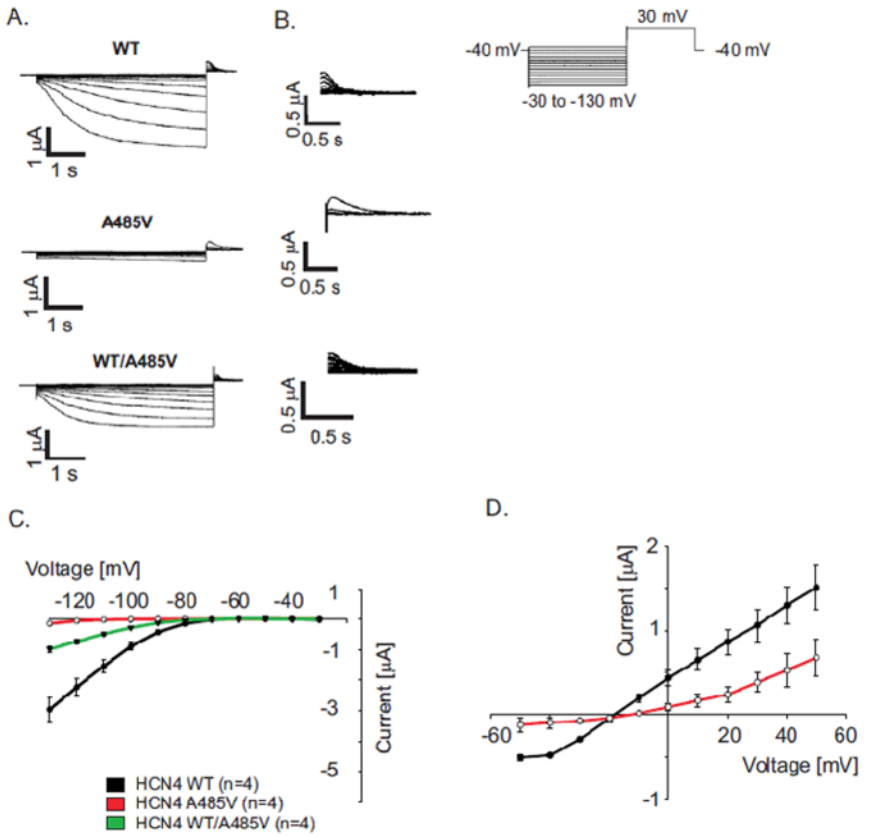

Figure 3. Results in *Xenopus* oocytes

Expression of HCN4 wild-type, HCN4 A485V homotetramer and HCN4 WT/A485V heterotetramer in *Xenopus* oocytes. **A.** Currents recorded from oocytes injected with RNAs of HCN4 WT, A485V, or WT and A485V together. The extracellular solution contained 24 mM K^+. **B.** Enlargement of traces of WT tail currents shown in A, recorded during the voltage step to 30 mV. *Right*, the voltage protocol. Holding potential was −40 mV and currents were elicited by 5-s hyperpolarizing voltage steps between −30 and −130 mV in 10-mV increments, followed by a 3-s step to 30 mV. **C.** I–V relationship of WT (full circles, n=4), A485V (empty circles, n=4) and HCN4 WT/A485V (full reverse triangles, n=4) channels, recorded at the end of the voltage steps between −30 and −130 mV. **D**. Reversal potential measurement of the HCN4 currents of WT (full circles, n=4) and A485V (empty circles, n=3). The measurement shows tail current amplitude at the indicated voltages after a 5-second pre-pulse to −130 mV. (**P*<0.05, same results obtained in two additional experiments).

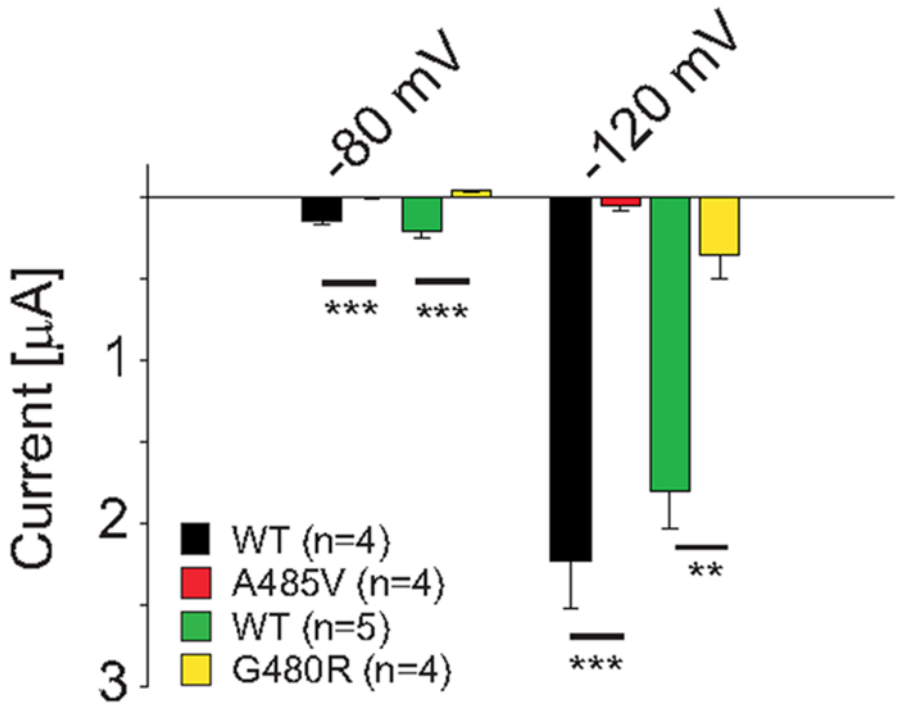

Figure 4. Comparison between the two mutations in the pore region

Comparison between HCN4 channels with A485V and G480R point mutations expressed in *Xenopus* oocytes. The currents of the HCN4 WT and homotetramer mutants were recorded in two separate experiments. The graph compares the currents of WT HCN4 (black, n=4) and A485V homozygote (red, n=4) to the currents of WT HCN4 (green, n=5) and G480R homozygote (yellow, n=4) at −80 mV, as well as at −120 mV. At −120 mV, the current of the homozygote mutants relative to the WT at the same experiment is 2.5 % and 20 % for A485V and G480R, respectively. (* $P<0.05$, ** $P<0.01$,*** $P<0.001$).

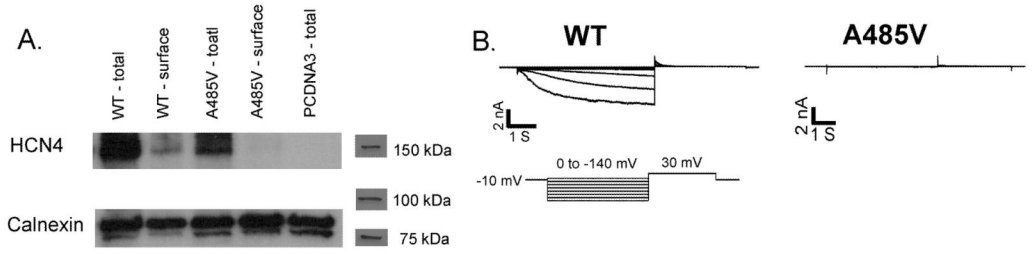

Figure 5. Results in HEK273T cells

Expression of HCN4 WT and HCN4 A485V homotetramers in HEK293T *cells*. A, Western blot of total protein using anti-HCN4 (top) or anti-Calnexin (bottom) antibodies in WT HCN4 transfected HEK293T cells, A485V HCN4 transfected cells and pCDNA3 transfected cells. Blot exposure time was 1 min. The area of each band was estimated using the Scion software, and was estimated as following: 11356 and 5716 for total HCN4 WT (*) and total A485V HCN4 (**), respectively. B, Currents recorded from cells transfected with DNA of HCN4 WT (n=4) or A485V (n=5). The extracellular solution contained 54 mM Na^+ and 90 mM K^+. *Right*, voltage protocol. Holding potential was −10 mV and currents were elicited by 5-s hyperpolarizing voltage steps between 0 and −140 mV in 20-mV increments.

Table 1

Baseline Clinical Characteristics of Family Members

			Holter Recording					Basic ECG parameters, ms		
Patient (Location in Pedigree)	**Sex**	**Age, y**	**Min**	**Avg**	**Max**	**Mutation Status (A485V)**	**Max HR achieved during exercise testing**	**PR**	**QRS**	**QTc**
A-I-4	F	76	35	59	93	Carrier	NA	200	80	392
A-II-2	F	52	37	62	154	Carrier	NA	120	80	367
A-II-4	M	57	41	72	138	Non-carrier	NA	200	100	393
A-II-5	F	58	39	57	102	Carrier	152	160	80	365
A-II-9	F	51	NA			Non-carrier	168	120	80	424
A-II-10	F	60	37	59	118	Carrier	149	160	80	390
A-II-12	M	62	38	60	116	Carrier	142	160	94	380
A-III-1	M	26	37	55	127	Carrier	175	140	80	426
A-III-2	F	19	36	59	103	Non-carrier	NA	160	60	450
A-III-4	F	29	45	83	148	Non-carrier	192	160	80	389
A-III-5*	M	21	33	53	162	Carrier	165	160	100	338
A-III-6	M	27	34	63	158	Carrier	194	160	80	400
A-III-7	F	14	62	91	190	Non-carrier	186	120	80	413
H-II-5	F	55	40	60	90	Carrier	NA	180	60	436
H-II-6	M	54	59	81	123	Non-carrier	163	160	60	402
H-III-1	M	22	31	49	92	Carrier	NA	120	80	367
H-III-2	F	28	43	64	129	Carrier	NA	160	60	367
H-III-3*	M	21	38	54	94	Carrier	170	160	60	340

			Holter Recording					Basic ECG parameters, ms		
Patient (Location in Pedigree)	**Sex**	**Age, y**	**Min**	**Avg**	**Max**	**Mutation Status (A485V)**	**Max HR achieved during exercise testing**	**PR**	**QRS**	**QTc**
H-III-4	M	27	38	70	122	Carrier	NA	160	80	367
V-II-2*	M	50	37	49	79	Carrier	186	160	60	406

*Index cases;

Table 2

Differences Between A485V Mutation Carriers and Non-carrier Family Members.

	A485V Carrier Family Members (n=14)	A485V Non-carrier Family Members (n=6)*	P value
Minimum heart rate	37 ± 3	49± 11	0.002
Average heart rate	58 ± 6	77 ± 12	0.0002
Maximum heart rate	117 ± 27	140 ± 32	NS
Average patient age	41.8 ± 19	37.3 ± 19	NS

* One non-carrier patient had illegible Holter recordings and therefore was excluded from the heart rate calculations.